Toxicon xxx (xxxx) xxx-xxx

Contents lists available at ScienceDirect

Toxicon

journal homepage: http://ees.elsevier.com

Bacterial expression of a snake venom metalloproteinase inhibitory protein from the North American opossum (*D. virginiana*)

R. Marshall Werner [a,*], Lauren M. Miling [a], Brianna M. Elliott [a], Mitchell R. Hawes [a], Jennifer M. Wickens [b,c], Danielle E. Webber [b,d]

[a] *Grand Valley State University, Department of Chemistry, 1 Campus Dr. 312 Padnos Hall, Allendale, MI, 49415, United States*
[b] *Lake Superior State University, Department of Chemistry, 650 W. Easterday Ave., Sault Ste. Marie, MI, 49583, United States*
[c] *Michigan State University College of Human Medicine, 965 Fee Rd A110, East Lansing, MI, 48824, United States*
[d] *Charles River Laboratories, 54943 N. Main St., Mattawan, MI, 49071, United States*

ARTICLE INFO

Handling Editor: Denise Tambourgi

Keywords
Snake venom metalloproteinase inhibitor
Didelphis virginiana
Oprin
DM43
Bacterial protein expression
Fluorescent peptide
Azocoll

ABSTRACT

A variety of opossum species are resistant to snake venoms due to the presence of antihemorrhagic and antimyotoxic acidic serum glycoproteins that inhibit several toxic venom components. Two virtually identical antihemorrhagic proteins isolated from either the North American opossum (*D. virginiana*) or the South American big-eared opossum (*D. aurita*), termed oprin or DM43 respectively, inhibit specific snake venom metalloproteinases (SVMPs). A better understanding of the structure of these proteins may provide useful insight to determine their mechanism of action and for the development of therapeutics against the global health concern of snake-bite envenomation. The aim of this work is to produce a recombinant snake venom metalloproteinase inhibitor (SVMPI) similar to the above opossum proteins in *Escherichia coli* and determine if this bacterially produced protein inhibits the proteolytic properties of Western Diamondback rattlesnake *(C. atrox*) venom. The resulting heterologous SVMPI was produced with either a 6-Histidine or maltose binding protein (MBP) affinity tag on either the C-terminus or N-terminus of the protein, respectively. The presence of the solubility enhancing MBP affinity tag resulted in significantly more soluble protein expression. The inhibitory activity was measured using two complementary assays and the MBP labeled SVMPI showed 7-fold less activity as compared to the 6-Histidine labeled SVMPI. Thus, the bacterially derived SVMPI with an unlabeled N-terminus showed high inhibitory activity (IC_{50} = 4.5 μM). The use of a solubility enhancing MBP fusion protein construct appears to be a productive way to express sufficient quantities of this mammalian protein in *E. coli* for further study.

1. Introduction

Envenomation by snakebite is a relevant public health concern in many regions of the world, particularly in tropical and subtropical regions, leading the World Health Organization to recognize this issue as a Neglected Public Health Issue in 2007(WHO, 2007; Williams et al., 2010). Though reliable global epidemiological data is scarce(Chippaux, 2017), between two to three million people are bitten by poisonous snakes annually, leading to an estimated 400,000 amputations and 125,000 fatalities(Gutiérrez et al., 2017; Williams et al., 2019).

Snake species responsible for the most bites and subsequent mortality include members of the Viperidae and Elapidae families(Warrell, 2010; Chippeau, 2017; Gutiérrez, 2017). Envenomation by viperid snakes (genus *Bothrops*, *Bitis*, *Crotalus*, *Daboia*, *Echis,* etc.) typically brings about significant local edema, hemorrhage, and necrosis coupled with myotoxicity and hemodynamic effects leading ultimately to cardiovascular shock and renal failure(Gutiérrez and Rucavado, 2000; Gutiérrez et al., 2005; Escalante et al., 2011a, 2011b; Markland and Swenson, 2013; Gasanov et al., 2014). Many of the effects of viperid venom are driven by the presence of large quantities of Ca^{2+}-dependent phospholipase A_2 myotoxins (PLA_2s), and a variety of Zn^{2+}-

Abbreviations: SVMP, snake venom metalloproteinase; SVMPI, snake venom metalloproteinase inhibitor; PLA_2, phospholipase A_2; SVSP, snake venom serine protease; 3FT, three-finger toxin; DTx, dendrotoxin; LTNF, lethal toxin neutralizing factor; IM, intramuscular; IV, intravenous; PCR, polymerase chain reaction; SDS-PAGE, sodium dodecyl sulfate polyacrylamide gel electrophoresis; MWCO, molecular weight cut-off; PVDF, polyvinylidene difluoride; EtBr, ethidium bromide; Amp, ampicillin; Kan, kanamycin; LB, Luria-Bertani culture media; IC_{50}, concentration of inhibitor that brings about 50 percent inhibition.

* Corresponding author. Grand Valley State University, Department of Chemistry, 1 Campus Dr. 312 Padnos Hall, Allendale, MI, 49415, United States.
E-mail address: wernerro@gvsu.edu (R. Marshall Werner)

https://doi.org/10.1016/j.toxicon.2021.01.008
Received 1 November 2020; Received in revised form 21 December 2020; Accepted 20 January 2021
Available online xxx
0041-0101/

dependent snake venom metalloproteinases (SVMPs) as well as snake venom serine proteases (SVSPs). Conversely, elapid venom (genus *Naja*, *Bungarus*, *Oxyuranus*, etc.) typically brings about neurotoxicity by targeting pre- and post-synaptic neuromuscular junctions, with some venoms also inducing localized necrosis and muscle breakdown (rhabdomyolysis). The effects of elapid venom are brought about by a high abundance of PLA_2s, and a variety of neurotoxins, most notably, the three-fingered toxins (3FTs) and dendrotoxin (DTx)(Gutiérrez et al., 2017). As a general rule, vipirid venom is considered to be more proteolytic, while elapid venom is more neurotoxic. The composition and evolution of snake venoms has recently been reviewed (Fox and Serrano, 2008; Calvete, 2017). For more than a century, immunoglobulin based antivenoms have been the primary treatment of systemic effects of snakebite envenoming(Gutiérrez et al., 2003; World Health Organization, 2010). However, unless administered rapidly after envenomation, antivenom may not prevent many of the tissue damaging effects caused by the presence of SVMPs, SVSPs and PLA_2s. Unfortunately, there currently is no treatment that can effectively ameliorate or reverse the destructive effects of these toxins(Gutiérrez et al., 2017). It has been suggested that a combination of SVMP and PLA_2 inhibitors, whether they be small molecules, peptidomimetics, or intact proteins, may provide an effective treatment for venom-induced tissue damage(Rucavado et al., 2000; Azofeifa et al., 2008; Villalta-Romero et al., 2012, 2017; Laustsen et al., 2016; Lewin et al., 2016; O'Brien et al., 2016).

A number of mammals exhibit resistance to both local and systematic effects of snake venoms. This natural resistance has been most studied in a variety of opossum (Didelphidae family) including the North American opossum (*D. virginiana*) and several South American opossum (*D. aurita*, *D. marsupialis*, *D. albiventris*, *L. crassicuadata*, *P. opossum*, and *P. frenatus*) and has been reviewed by a number of authors (Ovadia and Kochva, 1977; Perez and Sanchez, 1999; Voss and Jansa, 2012; Bastos et al., 2016). For further clarification on the everchanging systematics of the *Didelphidae* family, the reader is referred to a review by Gardner (2005)

In the 1940s, initial studies showed that several opossum species were resistant to a variety of venomous snakes(Vellard, 1945, 1949). Then, in the mid-1970s, researchers at the Edgewood Arsenal Biomedical Laboratory demonstrated the North American opossum (*D. virginiana*) is highly resistant to venom administered either intramuscularly (IM) or intravenously (IV) from a number of crotalid snake species(Kilmon, 1976; Werner and Vick, 1976, 1977). Additionally, it was demonstrated that *D. virginiana* possesses one or more inhibitory components in the serum, that confer resistance in mice to crotalid venom equal to or greater than the resistance conferred by commercial antivenin(Werner and Faith, 1978). While the title of this report indicated that the opossum species was *D. marsupialis*(Werner and Faith, 1978), it should be noted that the N. American opossum previously was identified as *D. marsupialis virginiana (Kerr)*(Gardner, 1973, 2005; Jurgelski, 1974), and it was confirmed that the species used in this study was in fact the N. American opossum, known now as *D. virginiana* (personal communication with author, Werner).

The first opossum-derived SVMPI protein was isolated from *D. virginiana* serum in 1979(Perez et al., 1979), but took until 1992 to be more fully characterized(Catanese and Kress, 1992). This inhibitory protein, coined "oprin" (for opossum inhibitor protein was also named as opossum α-1-β-glycoprotein), interacts with several SVMPs and inhibited *C. atrox* venom both *in vitro* and *in vivo*(Catanese and Kress, 1992). Other SVMPIs have subsequently been described from several South American opossum species, all with high sequence homology to oprin (Fig. 1)(Perales et al., 1994; Farah et al., 1996; Neves-Ferreira et al., 2000; Jurgilas et al., 2003). Interestingly, several recently published sequences from Australian marsupials such as the koala, wombat, and Tasmanian devil also show high sequence homology although the resistance of these animals to SVMPs is unclear.

The opossum SVMPIs studied thus far are glycosylated, but the role these moieties play in regard to function, folding, and solubility remain unclear. Interestingly, the SVMPI (DM43) from *D. aurita* (formerly *D. marsupialis*) (Gardner, 2005; (León et al., 2012)) retained half its activity when the glycan moieties were removed, suggesting that glycosylation may be required for cellular trafficking, solubility and correct protein folding but may be less important for inhibitory activity(León et al., 2012). In addition, there have been several reports indicating that short synthetic peptides corresponding to the first 10–15 amino acids of the N-terminal protein sequence of oprin termed LTNFs (lethal toxin neutralizing factors) inhibit SVMPs as well(Lipps, 1996; Lipps and Lipps, 1996; Lipps, 1999; Komives et al., 2017).

While a recent survey of structural studies of SVMPs and small molecule/peptide inhibitors provides useful information(Aoki-Shioi et al., 2020), further information regarding interactions of oprin-like proteins or short peptide SVMPIs with their target SVMP is limited to computer models(Chapeaurouge et al., 2009; Asega et al., 2014; Chavan and Deobagkar, 2014, 2015; Neves-Ferreira et al., 2002; Villalta-Romero et al., 2017), and attempts to crystalize these SVMPIs from opossum serum have thus far proven unsuccessful(Bastos et al., 2016). A better understanding of the molecular interactions involved between SVMPs and SVMPIs could provide useful information for the development of novel therapeutics for snake-bite envenomation(Bastos et al., 2016). This report describes our effort to express a recombinant oprin-like (DM43-like) protein from *D. virginiana* in *E. coli* utilizing ei-

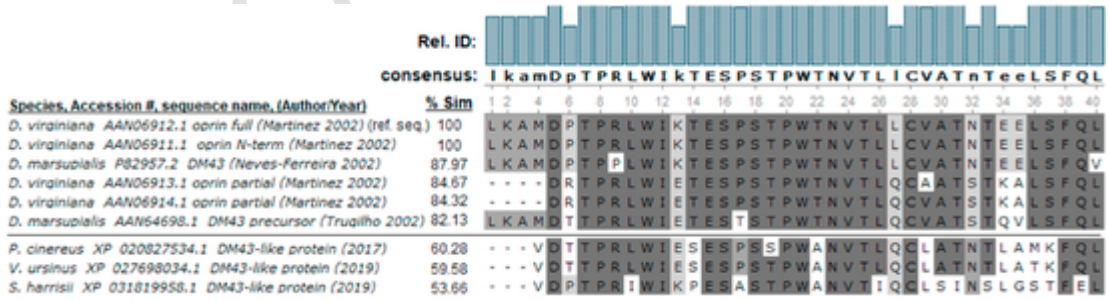

Fig. 1. Multiple protein sequence alignment for marsupial oprin and DM43-like SVMPI proteins showing the first 40 amino acids of a presumed consensus sequence. Darker grey shading indicates a position with higher sequence homology to the reference sequence (AAN06912.1). Capital letters in the consensus sequence have more than ninety percent homology between listed sequences while lower case letters have less than ninety percent homology. Bars labeled as "Rel. ID" indicate the relative number of sequences in the alignment with identical amino acids at a particular position, and percent identical similarity (% Sim) between sequences was generated using the National Center for Biotechnology Information (NCBI) protein BLASTP suite. Sequences 1 thru 6 are opossum (*Didelphis* genus) that were used to generate the consensus sequence while sequences 6 thru 8 (below solid line) are recently published Australian marsupial annotated genome derived sequences for the koala, wombat, and Tasmanian devil, respectively. The multiple sequence alignment was performed using the NCBI Multiple Alignment Sequence Viewer using the MUSCLE algorithm, and the figure was generated using Unipro UGENE software. (See supplemental for complete alignment and consensus sequence information.)

ther a 6-His or maltose binding protein (MBP) affinity tag to enhance purification and yield. Evidence is presented that these non-glycosylated proteins inhibit a variety of the proteolytic effects of Western Diamondback rattlesnake (*C. atrox*) venom *in vitro*. In addition to several lessons learned along the way, this work provides a pathway towards the large-scale production of these opossum-derived SVMPIs for mechanistic and structural studies.

2. Materials and methods

2.1. Reagents and materials

LB media, tryptone, yeast extract, agar, agarose, ethidium bromide, sodium chloride, calcium chloride, sodium phosphate, Tris-HCl, Tris base, ampicillin, kanamycin, EDTA (ethylenediamine tetraacetic acid), ethanol, methanol, DMSO (dimethylsulfoxide), DTT (dithiothreitol), and IPTG (Isopropyl β-D-1-thiogalactopyranoside) were obtained from Sigma (St. Louis, MO). pMAL Protein Fusion and Purification System (containing the pMAL-C5X plasmid and Factor X_a), NEBuilder HiFi DNA assembly 2X master mix, Q5 Hot Start High-Fidelity 2X Master Mix, OneTaq 2X Master Mix with standard buffer, NEB5-α competent *E. coli* (High Efficiency), NEBExpress competent *E. coli* (High Efficiency), Monarch Plasmid Miniprep Kit, Monarch DNA Gel Extraction Kit, CutSmart buffer 10X, restriction enzymes (XmnI, DpnI, BamHI-HF, NcoI-HF, XbaI), Purple 6X-load dye, and 1 KB Molecular Weight DNA ladder were obtained from New England Biolabs (NEB) (Ipswich, MA). Azocoll, Immobilon-P PVDF membrane, Amicon Ultra-15 (10K MWCO) centrifugal protein concentrators, pET28a plasmid, and BL21(DE3) competent *E. coli* cells were obtained from EMDMillipore (Burlington, MA). HiPur Ni-NTA Resin and HALT protease inhibitor were obtained from ThermoFisher Scientific (Waltham, MA). Anti-6xHis Mouse Monoclonal Antibody-HRP conjugate was from ProteinTech (Rosemont, IL). WesternBright ECL chemiluminescent HRP substrate and WesternBright peroxide were obtained from Advansta Corporation (Menlo Park, CA). All disposable plasticware and 96-well microplates were from VWR International (Radnor, PA). Mini-PROTEAN Tetra vertical electrophoresis cell, 4–20% Mini-PROTEAN TGX SDS-PAGE pre-cast protein gels, microcentrifuge tube roller, 10X Tris-Glycine SDS-PAGE buffer, 2X Laemmli sample buffer, protein assay dye concentrate (Bradford reagent), and Precision Plus Protein Kaleidoscope pre-stained protein molecular weight standard were from Bio-Rad (Hercules, CA). 2-aminobenzoyl-Ala-Gly-Leu-Ala-4-nitrobenzylamide (Abz-NGLA-Nbz) was obtained from Peptides International (Louisville, KY). Freeze-dried *Crotalus atrox* (*C. atrox*) venom was obtained from the National Natural Toxins Research Center at Texas A&M Kingsville. Synthetic desalted PCR primers (all primer sequences listed in the supplemental section) were obtained from Integrated DNA Technologies (Skokie, IL). A synthetic DNA encoding for the oprin DM43-like gene-product derived from a *D. virginiana* cDNA sequence (GenBank Accession number AY131001.1) inserted into the pUC19 vector was obtained from GeneScript Corporation (Piscataway, NJ). This pUC19-oprin construct contained HindIII restriction sites immediately upstream and downstream of the oprin coding sequence (876 bp) as well as an inserted TGA stop codon at the 3′-end of the sequence (see supplemental information for complete pUC19-oprin DM43-like vector sequence).

2.2. General methods

PCR was performed using specific primers (sequences listed in the supplemental section of this paper) and an Applied Biosystems Veriti thermocycler Model 9902 (ThermoFisher Scientific Waltham, MA), DNA visualization was performed using 0.8% agarose gels stained with EtBr and DNA concentration was measured with a microvolume UV spectrophotometer, namely the BioSpec-nano (Shimadzu Kyoto, Japan) or the NanoDrop2000 (ThermoFisher Scientific Waltham, MA). LB/Amp and LB/Kan liquid media and plates had final ampicillin and kanamycin concentrations of 100 mg/L and 30 mg/L, respectively. Proteins were concentrated using Amicon Ultra (10K MWCO) centrifugal concentrators. Protein concentrations were measured using either the Bio-Rad Bradford (1976) protein assay (Hercules, CA) or proteins were diluted in 8M guanidine hydrochloride followed by micro-cuvette UV–vis measurements using an Agilent Cary 60 UV–Vis spectrophotometer and calculated extinction coefficients (ExPASy ProtParam tool)(Gasteiger et al., 2005). Protein electrophoresis was performed with either a Bio-Rad (Hercules, CA) Mini-Protean 3 Cell or a Mini Trans-Blot Electrophoretic Transfer Cell. SDS-PAGE gels were stained with Coomassie blue stain. Micro-plate assays (for protein concentration and kinetic fluorescent assays) were performed using either a Spectramax M2^e microplate reader with Softmax Pro 5 software (Molecular Devices San Jose, CA) or a BioTek Synergy H1 Hybrid Reader (Winooski, VT). Chemiluminescent imaging was accomplished using a Li-Cor Odyssey infrared imaging system with Image Studio software (Li-Cor Biosciences Lincoln, NE). Centrifugation was accomplished using either a fixed angle VWR BenchMate micro-centrifuge, an Eppendorf 5417C microcentrifuge, a ThermoScientific Sorvall Lynx 400 fixed angle centrifuge, or a ThermoScientific Sorvall Legend X1 swinging bucket centrifuge. Sanger di-deoxy sequencing was performed at either Univeristy of Michigan Sequencing Core (Ann Arbor, MI) or Macrogen (Rockville, MD). IC_{50} values were calculated using GraphPad Prism version 8.4.2 for Windows, GraphPad Software (San Diego, CA)

2.3. Recombinant C-terminal 6-His-oprin protein

2.3.1. Gibson Assembly of C-terminal 6-His pET28a-oprin expression vector (Assembly 1)

To introduce overlapping oprin regions on both ends of the pET28a(+) vector (EMDMillipore), the vector was linearized using Q5 Hot Start High-Fidelity Polymerase 2X master mix with primers A and B (primer sequences provided in supplemental). A 25 μL PCR reaction contained: 12.5 μL of Q5 2X master mix, 1.25 μL of 10 μM primer A, 1.25 μL of 10 μM primer B, 1 μL of pET28a template DNA (1 pg), and 9 μL ultrapure H_2O. Thermocycler reaction conditions for the pET28a linearization reaction were: Stage 1: 60 sec 98 °C; Stage 2: 20 sec 98 °C, 30 sec 70 °C, 3 min 72 °C (35 cycles); Stage 3: 10 min 72 °C; Stage 4: 4 °C. To introduce overlapping pET28a regions on both ends of the oprin coding sequence, the appropriate region of the synthetic pUC19-oprin plasmid (Genescript) was amplified using Q5 Hot Start High-Fidelity Polymerase 2X master mix and primers C and D. A 25 μL PCR reaction contained: 12.5 μL of Q5 2X master mix, 1.25 μL of 10 μM primer C, 1.25 μL of 10 μM primer D, 0.5 μL of synthetic pUC19-oprin template DNA (0.1 ng), 9.5 μL ultrapure H_2O. Thermocycler reaction conditions for the oprin amplification reaction were: Stage 1: 60 sec 98 °C; Stage 2: 20 sec 98 °C, 30 sec 68 °C, 30 sec 72 °C (35 cycles); Stage 3: 10 min 72 °C; Stage 4: 4 °C. Assembly fragment lengths were verified by 0.8% agarose gel (stained with EtBr) (see supplemental), bands were excised, DNA was isolated using a Monarch DNA Gel Extraction Kit, and DNA concentration was determined using a micro-volume spectrophotometer. Prior to Gibson Assembly, linearized pET28a was treated with DpnI for 30 min at 37 °C in a reaction containing 8 μL (91 ng) of linearized pET28a, 1 μL of 10X CutSmart buffer, and 1 μL (20 units) of DpnI, followed by 20 min heat inactivation at 80 °C. Gibson Assembly conditions were as follows: 0.0125 pmol of the pET28a linearized fragment (vector) and 0.025 pmol of the oprin amplification fragment (insert) (~1:2 vector:insert ratio) were combined in a 20 μL assembly reaction with 10 μL of NEBuilder HiFi DNA 2X assembly master mix held at 50 °C for 30 min. NEB5-α competent cells (NEB) were transformed with 2 μL of the assembly reaction following the manufacture's 42 °C heat-shock protocol, incubated in SOC media at 37 °C for

60 min, and 100 μL was spread on LB/Kan agar plates and incubated at 37 °C overnight.

2.3.2. Colony PCR of Gibson Assembly transformation colonies

Colonies from Assembly 1 were screened by colony PCR using OneTaq 2X Master Mix with standard buffer and T7 promoter and terminator primers F and G. Eight colonies from the Gibson Assembly were randomly screened in separate 25 μL PCR reactions containing: 12.5 μL OneTaq, 1.25 μL of 10 μM primer F, 1.25 μL of 10 μM of primer G, 10 μL ultrapure H_2O, and individual colonies were picked with a sterile micro-pipette tip as the DNA source (note: these same tips were used to inoculate eight separate 10 mL LB/Kan liquid cultures grown overnight at 37 °C with shaking at 250 rpm). PCR thermocycler conditions for colony PCR were: Stage 1: 2 min 94 °C; Stage 2: 30 sec 94 °C, 30 sec 57 °C, 2 min 68 °C (35 cycles); Stage 3: 10 min 68 °C; Stage 4: 4 °C. Colony PCR results were visualized by 0.8% agarose gel (stained with EtBr) (see supplemental).

2.3.3. DNA isolation and sequencing

Plasmid DNA from the eight Assembly 1 transformation colonies was isolated from 1.5 mL of the LB/Kan liquid cultures of colonies showing appropriate amplicon length from colony PCR as visualized by 0.8% agarose gel (stained with EtBr) (see supplemental), using the Monarch Plasmid Miniprep Kit (NEB), eluted with 20 μL of elution buffer to give final plasmid DNA concentrations between 80 and 120 ng/μL as measured using a micro-volume spectrophotometer. Four of these purified plasmids were submitted for Sanger dideoxy-sequencing (University of Michigan Sequencing Core; Ann Arbor, MI) using primers F and G. Reads were trimmed and aligned (data not shown) using freeware FinchTV and UniProUGENE software (see supplemental for plasmid map and complete DNA and putative protein sequences)(FinchTV; Okonechnikov et al., 2012).

2.3.4. DNA restriction digest of Gibson Assembly 1

The pET28a-oprin construct from one of the sequenced Assembly 1 reactions was verified by a series of separate restriction digests containing either NcoI-HF, BamHI-HF, XbaI, XmnI, NcoI-HF + XbaI, NcoI-HF + XmnI, BamHI-HF + XmnI, or XbaI + XmnI. Digest reactions were performed at 37 °C and contained: 5 μL (~500 ng) DNA, 2 μL restriction enzyme (plus 2 μL of second restriction enzyme for double digests), 5 μL CutSmart 10X buffer (NEB), and an appropriate volume of ultrapure H_2O to bring the final volume to 50 μL. Reactions were stopped after 1 h by heating at 95 °C for 5 min, 10 μL of Purple 6X-load dye (NEB) was added to each reaction, and 10 μL of the restriction digest reactions were visualized with a 0.8% agarose gel (stained with EtBr) (see supplemental).

2.3.5. Transformation of C-terminal 6-His tag pET28a-oprin construct

The pET28a-oprin construct from Gibson Assembly 1 was transformed into BL21(DE3) *E. coli* cells (EMD Millipore) following the manufacture's protocol. The transformed cells (100 μL) were then spread onto LB/Kan plates and grown overnight at 37 °C.

2.3.6. Expression and purification of C-term 6-His-oprin protein

Four transformed colonies of BL21(DE3) *E. coli* containing the 6-His tag pET28a-oprin constructs from Assembly 1 were screened for IPTG-induced protein production by inoculating four separate 10 mL liquid LB/Kan media tubes containing 1 mM IPTG, incubated at 37 °C with overnight shaking at 250 rpm, and protein production was assessed via SDS-PAGE inspection. Once screened, the transformation colony showing the most IPTG-induced protein production was subjected to large-scale expression of the C-term 6-His-oprin protein. This was accomplished by inoculating two separate 2 L media flasks each containing 1 L of liquid LB/Kan media with 2 separate 5 mL portions of the starter culture of BL21(DE3) cells containing the previously screened Assembly 1 transformed colony. Cells were incubated at 37 °C with shaking at 250 rpm until the culture reached 0.5 OD_{600}, IPTG (final concentration of 1 mM) was added and the cells were incubated at 30 °C for an additional 4 h (Note: 30 °C incubation was found to give the most soluble protein, data not shown). The cells were harvested by centrifugation at 4000 G for 20 min at 4 °C, the supernatant was decanted, and the cell pellet was frozen at −20 °C overnight. The pellet was re-suspended in 25 mL lysis buffer (25 mM Tris-HCl pH 8, 400 mM NaCl, 10 mM imidazole, 1% glycerol) containing 10 mg lysozyme and 100 μL HALT protease inhibitor (Sigma). (Note: The addition of lysozyme and the protease inhibitor cocktail increased recovery of soluble MBP-oprin fusion protein significantly, data not shown). The sample was incubated at 37 °C for 10 min to induce cell lysis, sonicated with ten 30 s bursts at 25 Hz, and centrifuged at 15,000xg for 20 min at 4 °C. The supernatant was decanted and purified at 4 °C using approximately 5 cm^3 of HisPur Ni-NTA resin (ThermoScientific) according to the manufacture's protocol. The resin was equilibrated with 30 mL lysis buffer, the entire cell free lysate supernatant was applied via syringe to the column with a flow rate of 4.0 mL/min. The flow-through was re-applied to the resin two additional times to maximize binding. The column was washed twice using 10 mL of wash buffer (25 mM Tris-HCl pH 8, 400 mM NaCl, 25 mM imidazole, 1% glycerol) with a flow rate of 4.0 mL/min. The target protein was eluted in 1.2 mL fractions using elution buffer (25 mM Tris-HCl pH 8, 400 mM NaCl, 1 M imidazole, 1% glycerol) with a flow rate of 2.0 mL/min. Eluted fractions were examined for quantity and purity using the Bradford protein assay and SDS-PAGE, the fractions containing purified C-term 6-His oprin were pooled and exchanged into TNCT buffer (50 mM Tris-HCl pH 7.5, 150 mM NaCl, 1 mM $CaCl_2$, and 0.02% Tween-20) utilizing an Amicon 10,000 MWCO centrifugal concentrator (EMDMillipore). The sample was then brought to a final concentration of 1.0 mg/ml (~30 nM, based on a calculated molecular weight of 33,332 g/mol and a calculated extinction coefficient of 56,295 $M^{-1}cm^{-1}$) (values obtained from the ExPASy ProtParam tool)(Gasteiger et al., 2005). This buffer exchange was required to eliminate residual imidazole that can interfere with downstream inhibitor assays.

2.3.7. Western analysis of 6-His-oprin

Increasing quantities of purified 6-His-oprin (2 μg, 5 μg, 10 μg) as well as 50 μg of a 28.6 kDa 6-His-BshB reference protein (provided by Paul Cook, GVSU) were separated using an SDS-PAGE gel as described above. The gel was transferred to a PVDF membrane by electro-blotting following the manufacturer's recommendations (Bio-Rad). The membrane was then incubated in blocking buffer (PBST + 1% casein, 10 mM sodium phosphate pH 7.8, 150 mM NaCl, 0.05% v/v Tween-20) for 1 h at 25 °C, the blocking buffer was decanted, and 20 mL of a 1:10,000 fold dilution of a mouse 1° Anti-His-HRP conjugated antibody (ProteinTech) in blocking buffer was added for 1 h at 25 °C. The membrane was then rinsed three times for 5 min with PBST buffer and then incubated with 4 mL of a 1:1 mixture of WesternBright ECL chemiluminescent HRP substrate and WesternBright peroxide (Advansta) for 10 min and then imaged using an infrared imaging system (Li-Cor).

2.4. Recombinant N-terminal maltose binding protein-oprin (MBP-oprin) fusion protein

2.4.1. Gibson Assembly of MBP-oprin expression vector (Assembly 2)

To introduce overlapping oprin regions on both ends of the pMAL-C5x vector (New England Biolabs), the vector was linearized using Q5 Hot Start High-Fidelity Polymerase 2X master mix with primers H and I (primer sequences provided in supplemental). The 25 μL PCR reaction contained: 12.5 μL of Q5 2X master mix, 1.25 μL of 10 μM primer H, 1.25 μL of 10 μM primer I, 1 μL of pMAL-C5x template DNA (1 pg), and

9 μL ultrapure H_2O. PCR thermocycler reaction conditions for the construction of the pMAL-C5x assembly fragment were: Stage I: 30 sec 98 ºC; Stage 2: 5 sec 98 ºC, 30 sec 70 ºC, 5.0 min 72 °C (35 cycles); Stage 3: 10.0 min 72 °C; Stage 4: 4 °C. To introduce overlapping pMAL-C5x regions on both ends of the oprin coding sequence, the appropriate region of the synthetic pUC19-oprin plasmid (Genescript) was amplified using Q5 Hot Start High-Fidelity Polymerase 2X master mix and primers J and K. The 25 μL PCR reaction contained: 12.5 μL of Q5 2X master mix, 1.25 μL of 10 μM primer J, 1.25 μL of 10 μM primer K, 0.5 μL (1 pg) of synthetic pUC19-oprin template DNA, and 9.5 μL ultrapure H_2O. PCR thermocycler reaction conditions for the construction of the oprin assembly fragment were: Stage I: 30 sec 98 ºC; Stage 2: 5 sec 98 ºC, 30 sec 70 ºC, 45 sec 72 ºC (35 cycles); Stage 3: 3.0 min 72 °C; Stage 4: 4 °C. Assembly fragment lengths were verified by 0.8% agarose gel (stained with EtBr) (see supplemental), bands were excised, DNA was isolated using a Monarch DNA Gel Extraction Kit, and DNA concentration was determined using a micro-volume spectrophotometer. Prior to Gibson Assembly, linearized pMAL-C5x was treated with DpnI for 30 min at 37 °C in a reaction containing 8 μL (134 ng) of linearized pMAL-C5x, 1 μL of 10X CutSmart buffer, and 1 μL (20 units) of DpnI, followed by 20 min heat inactivation at 80 °C. Gibson Assembly conditions were as follows: 0.7 pmol of the pMAL-C5x linearized fragment (vector) and 1.4 pmol of the oprin assembly fragment (insert) (~1:2 vector/insert ratio) were combined in a 20 μL assembly reaction with 10 μL of NEBuilder HiFi DNA 2X assembly master mix and held at 50 °C for 15 min. NEB5-α competent *E. coli* cells (NEB) were then transformed with 2 μL of this assembly reaction following the manufacturer's 42 °C heat-shock protocol, incubated in SOC media at 37 °C for 60 min, and 100 μL was then spread on LB/Amp agar plates, and incubated at 37 °C overnight.

2.4.2. Colony PCR of Gibson Assembly transformation colonies

Colonies from Assembly 2 were screened by colony PCR in separate reactions using OneTaq 2X Master Mix with standard buffer and either oprin specific primers L and M (876 BP amplicon) or sequencing primers N and O (1137 BP amplicon) that amplify the oprin coding sequence with approximately 80 bp upstream and downstream extensions corresponding to the host pMAL-C5x vector. Eight colonies from the Gibson Assembly were randomly screened in separate 25 μL PCR reactions containing: 12.5 μL OneTaq, 1.25 μL of 10 μM primer L or N, 1.25 μL of 10 μM of primer M or O, and 10 μL ultrapure H_2O, and individual colonies were picked with a sterile micro-pipette tip as the DNA source (note: these same tips were used to inoculate separate 10 mL LB/Amp cultures grown overnight at 37 °C with shaking at 250 rpm. PCR thermocycler conditions for colony PCR were: Stage 1: 2 min 94 °C; Stage 2: 30 sec 94 ºC, 30 sec 57 ºC, 60 sec 68 ºC (35 cycles); Stage 3: 10 min 68 °C; Stage 4: 4 °C. Colony PCR results were visualized by 0.8% agarose gel (stained with EtBr) (see supplemental).

2.4.3. DNA isolation and sequencing

Plasmid DNA from the eight Assembly 2 transformation colonies was isolated from 1.5 mL of the LB/Amp liquid cultures of colonies showing appropriate amplicon lengths from colony PCR as visualized by 0.8% agarose gel (stained with EtBr, data not shown) using the Monarch Plasmid Miniprep Kit (NEB), eluted with 20 μL of elution buffer to give final plasmid DNA concentrations between 80 and 120 ng/μL as measured using a micro-volume spectrophotometer. Four of these purified plasmids were submitted for Sanger dideoxy-sequencing (Macrogen; Rockville, MD) using primers N and O. Reads were trimmed and aligned (data not shown) using freeware FinchTV and UniProUGENE software (see supplemental data for plasmid map and complete DNA and putative protein sequences)(FinchTV; Okonechnikov et al., 2012).

2.4.4. DNA restriction digest of Gibson Assembly 2

The pMAL-C5x-oprin construct from one of the sequenced Assembly 2 reactions was verified by a restriction digest with BamHI-HF (NEB). A 50 μL digest reaction contained: 5 μL (~500 ng) DNA, 2 μL restriction enzyme, of 5 μL CutSmart 10X buffer (NEB), and 38 μL of ultrapure H_2O. Reactions were stopped after 60 min by heating at 95 °C for 5 min, 10 μL of Purple 6X-load dye was added, and 10 μL of the restriction digest reaction was visualized with a 0.8% agarose gel (stained with EtBr) (see supplemental).

2.4.5. Transformation of MBP-oprin constructs

The pMAL-C5x-oprin construct from Assembly 2 was transformed into NEBExpress *E. coli* cells (NEB) following the manufacturer's protocol. This strain is recommended for the expression of MBP-fusion proteins because it is ideal for P_{tac} expression vectors such as pMAL-C5x and is deficient in proteases Lon and OmpT. The transformed cells (100 μL) were then spread onto LB/Amp plates and grown overnight at 37 °C.

2.4.6. Expression and purification of N-terminal MBP-Oprin fusion protein

Four transformed colonies of NEBExpress *E. coli* containing the N-terminal MBP-oprin constructs from Assembly 2 were screened for IPTG-induced protein production by inoculating four separate 10 mL liquid LB/Amp media tubes containing 1 mM IPTG, incubated at 37 °C with overnight shaking at 250 rpm, and protein production was assessed via SDS-PAGE inspection. Once screened, the transformation colony showing the most IPTG-induced protein production was subjected to large-scale expression of the N-terminal MBP-oprin protein. This was accomplished by inoculating 1 L of liquid LB/Amp/Glu (containing 1 mM glucose) media with a 10 mL starter culture of NEBExpress *E. coli* cells containing the previously screened Assembly 2 transformed colony. (Note: The addition of glucose is recommended as it inhibits the production of amylase, an enzyme that can degrade the amylose resin used in subsequent purification steps). Cells were initially incubated at 37 °C with shaking at 250 rpm until the cultures reached 0.4 OD_{600}, the temperature was then decreased to 30 °C, IPTG (final concentration of 1 mM) was added and the cells were incubated at 30 °C for an additional 6 h (Note: we found that if cultures were grown at 37 °C or for extended time periods, significant inclusion body formation was observed, data not shown). The cells were then harvested at 4000xg at 4 °C, the supernatant was decanted, and the cell pellets were frozen at −20 °C overnight. The cell pellets were re-suspended in a total of 60 mL of column buffer (20 mM Tris-HCl pH 7.4, 200 mM NaCl, 1 mM EDTA, and 0.5 mM DTT) containing 10 mg lysozyme and 100 μL HALT protease inhibitor (Sigma). (Note: The addition of lysozyme and the protease inhibitor cocktail increased recovery of soluble MBP-oprin fusion protein significantly, data not shown). The sample was incubated at 37 °C for 30 min to induce cell lysis, sonicated with ten 30 s bursts at 25 Hz, and centrifuged at 15,000xg for 20 min at 4 °C. The combined supernatants were decanted and purified at 4 °C using 40 cm^3 of amylose resin (NEB) equilibrated in column buffer with 1M NaCl added (Note: the addition of NaCl to the column buffer for equilibration and rinsing of the amylose column significantly reduced non-specific binding, see supplemental). A flow rate of 2.0 mL/min was used to rinse the column with 100 mL of column buffer with 1M NaCl added, and the MBP-oprin fusion protein was eluted into 3 mL fractions with column buffer containing 10 mM maltose but lacking the added 1M NaCl. Eluted fractions were examined for quantity and purity using the Bradford protein assay and SDS-PAGE, the fractions containing the purified MBP-oprin fusion protein were pooled and exchanged into TNCT buffer (50 mM Tris–HCl pH 7.5, 150 mM NaCl, 1 mM $CaCl_2$, and 0.02% Tween-20) utilizing a 10,000 MWCO centrifugal concentrator (EMDMillipore) to a final concentration of 5.0 mg/ml (~67 nM, based

on a calculated molecular weight of 75,001 g/mol and a calculated extinction coefficient of 122,245 $M^{-1}cm^{-1}$) (values obtained from the ExPASy ProtParam tool)(Gasteiger et al., 2005). This buffer exchange was required in our hands to eliminate residual EDTA and DTT, components that can interfere with downstream steps such as proteolytic cleavage or inhibitor assays.(Jenny et al., 2003; Waugh, 2011).

2.4.7. Cleavage of MBP-oprin with Factor X_a

Partial proteolytic cleavage of the MBP fragment was achieved by allowing 1 mg of Factor X_a (NEB) to react with a portion of the purified MBP-oprin fusion protein (250 μL, 1.25 mg) for 96 h at 0 °C (Note: a variety of conditions were examined to optimize cleavage, data not shown). The resulting cleavage reaction was analyzed by SDS-PAGE.

2.5. Collagenolytic inhibition assay

Azocoll (EMD Millipore) was used to evaluate collagenolytic activity of crude *C. atrox* venom and to evaluate the inhibitory activity of recombinant oprin proteins. The method of Pinto et al. was followed with modifications as described(Pinto et al., 2006). Crude *C. atrox* venom (1 g lyophilized powder) was dissolved in 5 mL ultrapure H_2O, and transferred to dialysis tubing, where it was exchanged with two separate 1 L volumes of TNCT buffer (50 mM Tris-HCl pH 7.5, 150 mM NaCl, 1 mM $CaCl_2$, and 0.02% Tween-20). The dialyzed crude venom was then diluted with TNCT buffer (500-fold dilution) and stored at −20 °C in 1.0 mL aliquots (Note: there was no measurable loss in activity after 6 months of storage using these conditions). A working stock of venom was made by adding 0.5 mL of this 500-fold diluted crude venom to 4.5 mL of TNCT buffer in a conical centrifuge tube (5000-fold dilution, called "Solution V"). A series of 2-fold serial dilutions of potential inhibitor proteins in TNCT buffer (either C-terminal 6-His-oprin or N-terminal MBP-oprin) were made in six separate 1.5 mL centrifuge tubes. In order to perform duplicate measurements, these inhibitor dilutions, along with the concentrated inhibitor stock (100 μL of each) were then mixed with 100 μL of Solution V in fourteen separate 1.5 mL microcentrifuge tubes and allowed to pre-incubate for 2 h at 37 °C. Additional duplicate incubation controls included 200 μL of TNCT buffer with no venom (negative control), 100 μL of TNCT buffer plus 100 μL Solution V (positive control), and 100 μL of 100 mM EDTA plus 100 μL Solution V (inhibitor control) (Note: several authors report that high concentrations of EDTA inhibit metalloproteinase venom components in similar assays) (Neves-Ferreira et al., 1997; León et al., 1998; Gay et al., 2005; Howes et al., 2007) In a separate 50 mL conical centrifuge tube, an Azocoll suspension (8 mg/mL) was made by vortexing 360 mg of Azocoll in 45 mL of TNCT buffer. The Azocoll substrate (100 μL) was then added to each of the inhibitor/venom pre-incubates and controls described above and placed on a tube roller (Bio-Rad) with gentle rotation at 37 °C for 4 h (Note: it was found that the Azocoll suspension must be mixed by inversion before each addition for consistent results, and that the use of a tube roller was superior to a bio-shaker at high rpm). The reactions were centrifuged at 13,000xg for 1 min at 25 °C to pellet the remaining insoluble Azocoll substrate, 200 μL of supernatant from each reaction was transferred to a 96-well microplate, and the absorbance was measured at 550 nm. For this non-continuous assay, the percent of remaining venom activity at differing inhibitor concentrations was calculated by dividing the absorbance for each sample by the maximal absorbance obtained when venom was present but no inhibitor was present (positive control). This data was normalized using values for the positive control (no inhibitor – maximal activity) as the upper curve boundary and average values for both the negative control (no venom) and the inhibitor control (EDTA) as the lower curve boundary. Non-linear regression was applied to the log[inhibitor] vs. normalized response dose-response curves using a variable slope method, and IC_{50} values were derived from this curve using GraphPad Prism software.

2.6. Continuous fluorescent peptide hydrolysis inhibition assay

The fluorescent peptide substrate (Abz-AGLA-Nbz), has been utilized as an effective substrate to determine kinetic parameters of a variety of proteases as well as SVMPs and their associated inhibitors(Nishino and Powers, 1980; Rush et al., 1984; Neves-Ferreira et al., 2000; Jurgilas et al., 2003; Villalta-Romero et al., 2012). A portion of an 8 mM Abz-AGLA-Nbz dissolved in a H_2O:DMSO (9:1) stock solution was diluted 200-fold (0.04 mM final concentration) in TNCT buffer (50 mM Tris-HCl pH 7.5, 150 mM NaCl, 1 mM $CaCl_2$, and 0.02% Tween-20) in a 40 mL plastic trough. Venom/inhibitor pre-incubates and controls that were prepared as described for the collagenolytic assay (section 2.5) were used for this experiment and were pre-incubated for 2 h at 37 °C. Black 96-well plates were used to perform triplicate measurements. Abz-AGLA-Nbz (100 μL of the 0.04 mM diluted stock) was added to 30 wells of the microplate using a multichannel pipettor. The pre-incubates and controls (170 μL) were first added to empty wells of the microplate and then a multichannel pipettor was used to initiate the reactions by transferring 50 μL of these to the wells already containing the Abz-AGLA-Nbz substrate. The plate was then read at 37 °C using excitation and emission wavelengths of 340 nm and 415 nm, respectively, for 10 min at 30 s intervals. For this continuous assay, the initial slopes of these kinetic measurements were used to determine the percent of remaining venom activity at differing inhibitor concentrations by dividing the initial slopes for each sample by the maximal slope obtained when no inhibitor was present (positive control). This data was normalized using values for the positive control (no inhibitor – maximal activity) as the upper curve boundary and average values for both the negative control (no venom) and the inhibitor control (EDTA) as the lower curve boundary. Non-linear regression was applied to the log[inhibitor] vs. normalized response dose-response curves using a variable slope method, and IC_{50} values were derived from this curve using GraphPad Prism software.

3. Results and discussion

3.1. Bacterial production of recombinant SVMPIs

The production of soluble mammalian proteins using recombinant expression vectors in bacteria can be both challenging and rewarding. Mammalian proteins typically contain post-translational modifications (i.e. glycosylation, signal sequence cleavage) that are not found in bacterial systems(Altenbuchner and Mattes, 2006). These issues can often lead to the production of proteins in bacteria that are neither soluble nor active, and can limit the use of this approach(Hochkoeppler, 2013). However, the production of mammalian proteins in bacteria, most notably *E. coli*, for structural and functional studies has a rich history and remarkable success rate(Sahdev et al., 2008). The use of affinity tags as well as solubilization fusion proteins has increased the successful production of mammalian proteins in bacteria significantly(Yang et al., 2016).

In response to the call for additional methods to understand the interaction of mammalian SVMPIs and their target SVMPs(Bastos et al., 2016), we expressed a SVMPI protein derived from the N. American opossum (*D. virginiana*), originally termed "oprin" and subsequently shown to be highly homologous to DM43(Neves-Ferreira et al., 2002), utilizing two approaches involving an affinity fusion tag. First, we investigated the production of a C-terminal 6-His tagged oprin protein using a pET-series vector, namely pET28a(+). Second, we investigated the production of an N-terminal maltose binding protein (MBP) tagged oprin protein to evaluate the ability of MBP to improve solubility of these recombinant proteins using the pMAL-C5x vector. A cDNA

derived sequence that encodes for the oprin protein (GenBank AY131001.1) was chemically synthesized and produced in a pUC19 vector. Appropriate overlapping ends were added to the coding sequence using PCR and then inserted into the above linearized expression vectors with corresponding overlapping ends using the Gibson Assembly procedure(Gibson et al., 2009). The insertion of the oprin sequence into either pET28a(+) (Assembly 1) or pMAL-C5x (Assembly 2) using Gibson Assembly was straightforward as was the characterization and sequencing of these DNA constructs (see supplemental).

The expression of C-terminal 6-His-oprin was accomplished by transforming BL21(DE3) *E. coli* cells with the pET28a(+)-oprin construct (Assembly 1). Upon the addition of IPTG to large cultures entering the exponential growth phase, the 6-His-oprin protein (~33 kDa) was produced (Fig. 2A). Unfortunately, regardless of the growth conditions tested, the majority of this protein was produced as insoluble inclusion bodies as visualized by comparing the "lysate super" and "lysate pellet" lanes in Fig. 2A. Attempts to resolubilize the pellet were moderately successful, however, these fractions showed no inhibitory activity of *C. atrox* venom suggesting that improper protein folding and aggregation may have occurred (data not shown). When the soluble cell lysate supernatant fraction was subjected to affinity purification using a HisPur Ni-NTA column, the 6-His-oprin was purified in relatively small quantities upon elution from the column with imidazole (~10 mg from 2 L of culture) as visualized in Fig. 2B. An approximate molecular weight of 33 kDa as well as the presence of the 6-His affinity tag was verified by Western blot analysis (Fig. 2C).

The expression of N-terminal MBP-oprin was accomplished by transforming NEBExpress *E. coli* cells with the pMAL-C5x-oprin construct (Assembly 2). Upon the addition of IPTG to a large culture entering the exponential growth phase, the MBP-oprin protein (~75 kDa) was produced (Fig. 3A). Fortunately, the majority of this protein was produced in the soluble "lysate super" fraction as compared to the insoluble "lysate pellet" fraction. These results contrasted with those found for the 6-His-oprin protein that tended to express as insoluble inclusion bodies. When the soluble cell lysate supernatant fraction was subjected to affinity purification using an amylose column, the MBP-oprin was purified in relatively large quantities (~40 mg from 1 L culture) upon elution from the column with maltose as visualized in Fig. 3A. The Factor X_a cleavage of the MBP-oprin fusion (~75 kDa) yielding the oprin protein (~33 kDa) and MBP (~42 kDa) was ultimately accomplished in low yield, but only after a prolonged reaction time of 96 h at 25 °C (Fig. 3B). Attempts to optimize or further prolong the cleavage reaction had limited success and led to additional non-specific proteolysis (data not shown). Attempts to purify the liberated oprin protein were unsuccessful.

3.2. Inhibitory activity of recombinant SVMPIs

The inhibitory activity of the C-Term-6-His-oprin (from Assembly 1) and the N-Term-MBP-oprin (from Assembly 2) were assessed using two different *in vitro* methods. First, the ability of these SVMPIs to inhibit crude *C. atrox* venom mediated hydrolysis of collagen was measured in

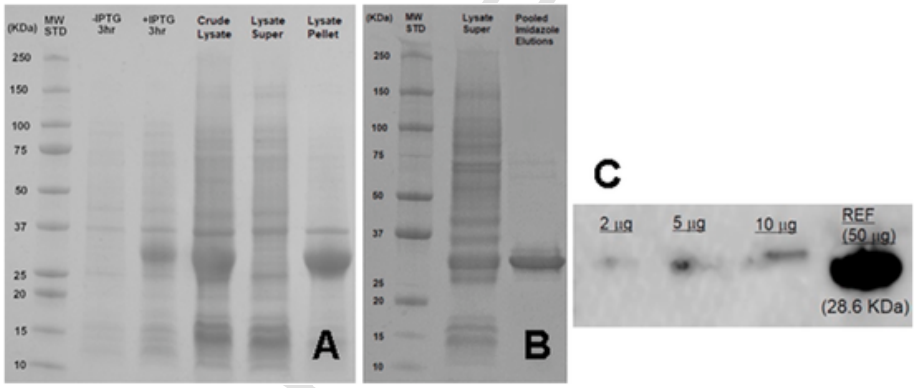

Fig. 2. A. SDS-PAGE gel showing the expression of 6-His-oprin (~33 kDa) (Coomassie blue stain). **B**. SDS-PAGE gel showing the purification of 6-His-oprin from the crude cell lysate using a HisPur Ni-NTA affinity column (Coomassie blue stain). **C**. Immunoblot derived from an SDS-PAGE gel showing the Western analysis of increasing amounts of 6-His-oprin (2 µg, 5 µg, 10 µg) compared to 50 µg of a 28.6 KDa 6-His reference protein, 6-His-BshB (chemiluminescent image using WesternBright ECL substrate/peroxide and Anti-His-6-HRP congugate 1° antibody).

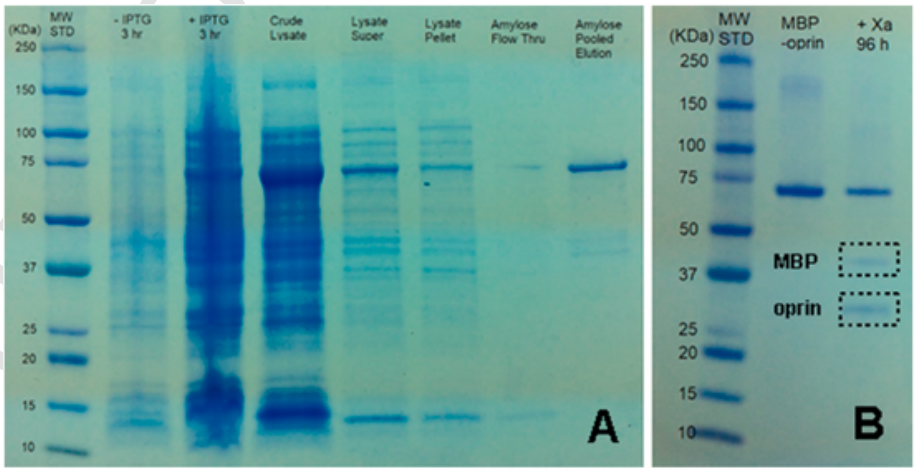

Fig. 3. A. SDS-PAGE gel showing the expression and purification of MBP-oprin (Coomassie Blue stain). **B**. SDS-PAGE gel showing the Factor X_a cleavage of MBP-oprin (~75 kDa) to MBP (~42 kDa) and oprin (~33 kDa) (Coomassie Blue stain). (For interpretation of the references to color in this figure legend, the reader is referred to the Web version of this article.)

a pre-incubation non-continuous assay using the commercially available reagent Azocoll, an azo-labeled collagen that is used in studies on a variety of proteases(Moore, 1969; Chavira et al., 1984; Biardi et al., 2006; Pinto et al., 2006 Fernandes et al., 2014). Second, inhibition studies were performed in a pre-incubation continuous assay using the commercially available fluorogenic peptide, Abz-AGLA-Nbz, a peptide that is used to study a variety of SVMPs(Neves-Ferreira et al., 2000; Jurgilas et al., 2003; Villalta-Romero et al., 2012). In both of these assays, EDTA was used as an inhibitor control as high concentrations completely inhibit metalloprotease mediated peptide hydrolysis by crude *C. atrox* venom in these assays(Price, 2015). The dose-response curves used for the determination of IC_{50} values and associated parameters for these SVMPIs are shown in Fig. 4 and summarized in Table 1.

The IC_{50} values determined using two different *in vitro* methods in this study were within a factor of three, thus, average IC_{50} values derived from the two methods for the C-Term-6-His-oprin (4.5 μM) and the N-Term-MBP-oprin (32.5 μM) are suggested with reasonable confidence. It is important to note that in these assays, inhibitor and venom were pre-incubated for 2 h, thus these results do not represent actual IC_{50} values for *in vivo* experiments where the SVMPI might be administered post envenomation. In addition, these assays do not control for proteolytic cleavage by other components of C. atrox venom (i.e. serine proteases) and thus may represent an underestimate of the inhibitory effects these recombinant proteins may have on SVMPs. However, the 7-fold reduction in the inhibitory activity of the N-terminal MBP-labeled oprin relative to the C-terminal 6-histidine labeled inhibitor suggests that the amino-terminus of this SVMPI may play a *more* important role in forming a complex between the SVMPI and its target SVMP in venom.

It has been demonstrated that the SVMP:SVMPI complex has a 1:1 stoichiometry, at least for jararhagin (the main hemorrhagic metalloproteinase from *B. jararaca* venom) complexed with either of the highly analogous SVMPIs (DM43 or PO41) derived from the South American opossums *D. marsupilais (now referred to as D. aurita)* or *P. opossum,* respectively(Neves-Ferreira et al., 2002; Jurgilas et al., 2003). Because the current studies looked at inhibition of crude venom rather than isolated metalloproteinases, the stoichiometry of the SVMP:SVMPI complex was not determined but rather inferred due to homology. Furthermore, it is recognized that the N-terminus of the opossum SVMPIs have high sequence homology (Fig. 1), and that 10-15mer peptides with this N-terminal sequence, termed lethal toxin neutralizing factors (LTNFs)(Lipps, 1996), also act as moderately effective SVMPIs(Komives et al., 2017). The presence of a 6-His affinity tag on the C-terminus may reduce inhibition relative to a "native" oprin protein, but additional studies would be needed to investigate this possibility. While having a free amino-terminus appears to be important in forming the SVMP:SVMPI complex, the results presented here indicate that this is not an absolute requirement for inhibition.

Finally, because bacterially derived proteins are not glycosylated, the question arises as to the role of the glycan moities in the native opossum SVMPI. Previous studies demonstrated that when these glycan units were removed, the inhibitory activity of DM43 towards jararhagin was reduced by half suggesting an important role for these moieties(León et al., 2012). Likewise, studies of a related protein, an opossum (*D. aurita*) phospholipase A_2 (PLA_2) inhibitor (DM64) expressed in *P. pastoris*, demonstrated that this recombinant protein exhibited inhibitory activity even though it did not have the native complement of sugars or when the glycans were removed(León et al., 2012; Vieira et al., 2017). The current studies showing that the C-Term-6-His-oprin when grown in bacteria is expressed almost exclusively as inclusion bodies while the MBP-oprin is expressed primarily in soluble form, indicate that glycosylation may play a *more* important role in protein solubilization and folding rather than crucial interactions in the SVMP:SVMPI complex. Another potential role for these sugars is the stabilization of dimers between these opossum SVMPIs(Neves-Ferreira et al., 2002; Brand et al., 2012), a possibility that the current study did not address.

4. Conclusion

This study demonstrates the feasibility of expressing functionally active mammalian SVMPIs derived from *D. virginiana* in *E. coli*, a prospect that will aid in the further investigation of the structural characteristics that allow them to inhibit their target SVMPs. The use of a solubility enhancer such as the maltose binding protein (MBP) may allow for sufficient quantities of these proteins to be produced to achieve these goals. We are currently working on improving our solubilization enhancer-oprin fusion protein design to increase yield and allow for easier cleavage of the fusion protein. We hope to couple these approaches with site-directed mutagenesis and x-ray crystallographic structural studies to identify the critical protein regions necessary for inhibition of SVMPs.

Credit authorship

R. Marshall Werner: Conceptualization, Methodology, Validation, Formal Analysis, Investigation, Writing – Original, Visualization, Supervision, Project Administration, Funding acquisition; Lauren M. Miling: Investigation, Funding acquisition, Writing – Review & Editing; Brianna M. Elliot: Investigation; Mitchell R. Hawes: Investigation; Jennifer M. Wickens: Investigation, Funding acquisition, Writing – Review & Editing; Danielle E. Webber: Investigation, Writing – Review & Editing.

Ethical statement

The authors agree to all ethical and authorship guidelines as outlined by Elsevier Publishing and the journal Toxicon found at the following link: https://www.elsevier.com/about/policies/publishing-

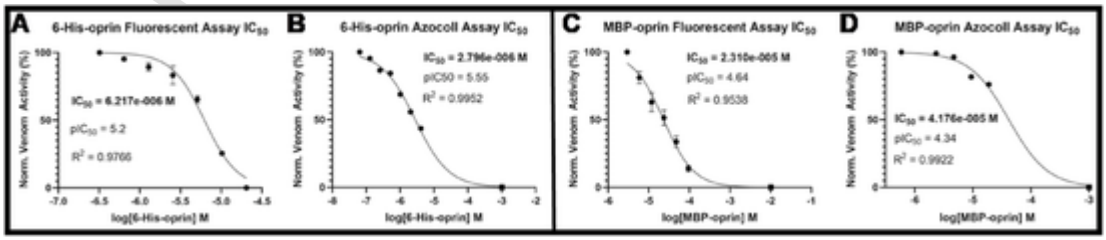

Fig. 4. Normalized dose-response curves used for the determination of the IC_{50} values for the SVMPIs 6-His-oprin and MBP-oprin against crude *C. atrox* venom. A and B show the curves for 6-His-oprin utilizing either the fluorescent or Azocoll assays, respectively. C and D show the curves for MBP-oprin utilizing either the fluorescent or Azocoll assays, respectively. Experimental data points are shown with black circles. Curves B, C, and D were normalized relative to a maximal activity when no inhibitor was present (data points not shown, negative control) or to minimal activity when 100 mM EDTA was present (square data point, inhibitor control). The minimal activity of Curve A was normalized to an experimental data point with the highest inhibitor concentration. The IC_{50} values are reported in molar (M) units, $pIC_{50} = -\log(IC_{50})$ where R^2 is the coefficient of determination relative to the curve derived using non-linear regression with a value of one representing an ideal fit.

Table 1
Summary of IC_{50} values and associated parameters determined for the SVMPIs 6-His-oprin and MBP-oprin on crude *C. atrox* venom using either the fluorescent peptide or Azocoll assay using the equation pIC_{50} = -log(IC_{50} where R^2 is the coefficient of determination relative to the curve derived using non-linear regression with a value of one representing an ideal fit. Average IC_{50} values represent the average of the two different measurement methods.

SVMPI	Assay	IC_{50} (μM)	Avg. IC_{50} (μM)	pIC_{50}	Avg. pIC_{50}	R^2
C-Terminal 6-His-oprin	Fluorescent	6.2	4.5	5.2	5.38	0.9766
C-Terminal 6-His-oprin	Azocoll	2.8		5.55		0.9952
N-Terminal MBP-oprin	Fluorescent	23.1	32.5	4.64	4.49	0.9538
N-Terminal MBP-oprin	Azocoll	41.8		4.34		0.9922

ethics.

Declaration of competing interest

The authors declare that they have no known competing financial interests or personal relationships that could have appeared to influence the work reported in this paper.

Acknowledgements

We would like to thank Dr. Robert M. Werner, DVM (corresponding author's father) for his assistance with historical insights regarding his work on the resistance of *D. virginiana* to snake venom in the mid-1970s at Edgewood Arsenal Biomedical Laboratory as well as his clarification regarding the naming of *D. virginiana* as it was also referred to as *D. marsupialis virginiana (Kerr)* in the mid-1970s (personal communication). LM thanks Grand Valley State University for undergraduate research funding, while JW thanks Lake Superior State University for undergraduate research funding. The authors also wish to thank students from Lake Superior State University who participated in several portions of this research as part of an advanced biochemistry class. The 6-His-BshB protein used as a reference for Western analysis was kindly provided by Paul Cook (GVSU), and we thank David Leonard (GVSU) for assistance with laboratory research space.

Appendix A. Supplementary data

Supplementary data related to this article can be found at https://doi.org/10.1016/j.toxicon.2021.01.008.

Uncited reference

Catanese and Kress, 1993.

References

Altenbuchner, J., Mattes, R., 2006. Escherichia coli. In: Gellissen, G. (Ed.), Production of Recombinant Proteins: Novel Microbial and Eukaryotic Expression Systems. John Wiley & Sons, NY, pp. 7–37.

Aoki-Shioi, N., Koh, C.Y., Kini, R.M., 2020. Natural inhibitors of snake venom metalloproteinases. Aust. J. Chem. 73, 277–286. doi:10.1071/ch19414.

Asega, A.F., Oliveira, A.K., Menezes, M.C., Neves-Ferreira, A.G.C., Serrano, S.M.T., 2014. Interaction of *bothrops jararaca* venom metalloproteinases with protein inhibitors. Toxicon 80, 1–8. doi:10.1016/j.toxicon.2014.01.001.

Azofeifa, K., Angulo, Y., Lomonte, B., 2008. Ability of fucoidan to prevent muscle necrosis induced by snake venom myotoxins: comparison of high- and low-molecular weight fractions. Toxicon 51, 373–380. doi:10.1016/j.toxicon.2007.10.008.

Bastos, V.A., Gomes-Neto, F., Perales, J., Neves-Ferreira, A.G.C., Valente, R.H., 2016. Natural inhibitors of snake venom metalloendopeptidases: history and current challenges. Toxins 8, 250–279. doi:10.3390/toxins8090250.

Biardi, J.E., Chien, D.C., Coss, R.G., 2006. California ground squirrel (*spermophilus beecheyi*) defenses against rattlesnake venom digestive and hemostatic toxins. J. Chem. Ecol. 32, 137–154. doi:10.1007/s10886-006-9357-8.

Bradford, M.M., 1976. A rapid and sensitive method for the quantitation of microgram quantities of protein utilizing the principle of protein-dye binding. Anal. Biochem. 72, 248–254. doi:10.1016/0003-2697(76)90527-3.

Brand, G.D., Salbo, R., Jørgensen, T.J.D., Bloch, C., Erba, E.B., Robinson, C.V., Tanjoni, I., Moura-da-Silva, M., Roepstorff, P., Domont, G.B., Perales, J., Valente, R.H., Neves-Ferreira, A.G.C., 2012. The interaction of the antitoxin DM43 with a snake venom metalloproteinase analyzed by mass spectrometry and surface plasmon resonance. J. Mass Spectrom. 47, 567–573. doi:10.1002/jms.2990.

Calvete, J.J., 2017. Venomics: integrative venom proteomics and beyond. Biochem. J. 474, 611–634. doi:10.1042/BCJ20160577.

Catanese, J.J., Kress, L.F., 1992. Isolation from opossum serum of a metalloproteinase inhibitor homologous to human α-1-β-glycoprotein. Biochemistry 31, 410–418. doi:10.1021/bi00117a015.

Catanese, J.J., Kress, L.F., 1993. Opossum serum α-1-proteinase inhibitor: purification, linear sequence, and resistance to inactivation by rattlesnake venom metalloproteinase. Biochemistry 32, 509–515. doi:10.1021/bi00053a015.

Chapeaurouge, A., Martins, S.M., Holub, O., Rocha, S.L.G., Valente, R.H., Neves-Ferreira, A.G.C., Ferreira, S.T., Domont, G.B., Perales, J., 2009. Conformational plasticity of DM43, a metalloproteinase inhibitor from *didelphis marsupialis*: chemical and pressure-induced equilibrium (un)folding studies. Biochim. Biophys. Acta Protein Proteonomics 1794, 1379–1386. doi:10.1016/j.bbapap.2009.03.010.

Chavan, S.G., Deobagkar, D.D., 2014. *In silico* molecular interaction analysis of LTNF peptide-LT10 with snake venom enzymes. Protein Pept. Lett. 21, 646–656 URL (accessed 10/19/2020): https://www.ingentaconnect.com/content/ben/ppl/2014/00000021/00000007/art00006.

Chavan, S.G., Deobagkar, D.D., 2015. An *in silico* insight into novel therapeutic interaction of LTNF peptide-LT10 and design of structure based peptidomimetics for putative anti-diabetic activity. PloS One 10, e0121860. doi:10.1371/journal.pone.0121860.

Chavira, R., Burnett, T.J., Hageman, J.H., 1984. Assaying proteinases with azocoll. Anal. Biochem. 136, 446–450. doi:10.1016/0003-2697(84)90242-2.

Chippaux, J.P., 2017. Incidence and mortality due to snakebite in the Americas. PLoS Neglected Trop. Dis. 11, e0005662. doi:10.1371/journal.pntd.0005662.

Escalante, T., Ortiz, N., Rucavado, A., Sanchez, E., Richardson, M., Fox, J., Gutiérrez, J., 2011a. Role of collagens and perlecan in microvascular stability: exploring the mechanism of capillary vessel damage by snake venom metalloproteinases. PloS One 6, e28017. doi:10.1371/journal.pone.0028017.

Escalante, T., Rucavado, A., Fox, J.W., Gutiérrez, J.M., 2011b. Key events in microvascular damage induced by snake venom hemorrhagic metalloproteinases. J. of Proteomics. 74, 1781–1794. doi:10.1016/j.jprot.2011.03.026.

Farah, M.D.F.L., One, M., Novello, J.C., Toyama, M.H., Perales, J., Moussatché, H., Domont, G.B., Oliveira, B., Marangoni, S., 1996. Isolation of protein factors from opossum (*Didelphis albiventris*) serum which protect against *Bothrops jararaca* venom. Toxicon 34, 1067–1071. doi:10.1016/0041-0101(96)00034-7.

Fernandes, F.F.A., Tomaz, M.A., El-Kik, C.Z., Monteiro-Machado, M., Strauch, M.A., Cons, B.L., Tavares-Henriques, M.S., Cintra, A.C.O., Facundo, V.A., Melo, P.A., 2014. Counteraction of bothrops snake venoms by *combretum leprosum* root extract and arjunolic acid. J. Ethnopharmacol. 155, 552–562. doi:10.1016/j.jep.2014.05.056.

FinchTV. FinchTV 1.4.0 (Geospiza, Inc.; Seattle, WA, USA); URL accessed (7/2/2020): https://digitalworldbiology.com/finchtv.

Fox, J.W., Serrano, S.M.T., 2008. Exploring snake venom proteomes: multifaceted analyses for complex toxin mixtures. Proteomics 8, 909–920. doi:10.1002/pmic.200700777.

Gasanov, S.E., Dagda, R.K., Rael, E.D., 2014. Snake venom cytotoxins, phospholipase A_2s, and Zn(2+)-dependent metalloproteinases: mechanisms of action and pharmacological relevance. J. Clin. Toxicol. 4, 1000181. doi:10.4172/2161-0495.1000181.

Gasteiger, E., Hoogland, C., Gattiker, A., Duvaud, S., Wilkins, M.R., Appel, R.D., Bairoch, A., 2005. Protein identification and analysis tools on the Expasy server. In: Walker, J.M. (Ed.), The Proteomics Protocols Handbook. Humana Press, Totowa, NJ, pp. 571–607.

Gardner, A.L., 1973. The systematics of the genus *Didelphis* (marsupialia: didelphidae) in North and Middle America. In: Special Publ, No. 4. Museum of Texas Tech Univ., Lubbock, TX.

Gardner, A.L., 2005. In: Wilson, D.E., Reeder, D.M. (Eds.), Order Didelphimorphia in Mammal Species of the World, 3rd ed. Johns Hopkins University Press, Baltimore, MD, pp. 3–18.

Gay, C.C., Leiva, L.C., Maruñak, S., Teibler, P., Acosta de Pérez, O., 2005. Proteolytic, edematogenic and myotoxic activities of a hemorrhagic metalloproteinase isolated from *Bothrops alternatus* venom. Toxicon 46, 546–554. doi:10.1016/j.toxicon.2005.06.019.

Gibson, D.G., Young, L., Chuang, R.Y., Venter, J.C., Hutchison, C.A., Smith, H.O., 2009. Enzymatic assembly of DNA molecules up to several hundred kilobases. Nat. Methods 6, 343–345. doi:10.1038/nmeth.1318.

Gutiérrez, J.M., Calvete, J.J., Habib, A.G., Harrison, R.A., Williams, D.J., Warrell, D.A., 2017. Snakebite envenoming. Nature Reviews Disease Primers 3, 17063. doi:10.1038/nrdp.2017.63.

Gutiérrez, J.M., León, G., Lomonte, B., 2003. Pharmacokinetic-pharmacodynamic relationships of immunoglobulin therapy for envenomation. Clin. Pharmacokinet. 42, 721–741. doi:10.2165/00003088-200342080-00002.

Gutiérrez, J.M., Rucavado, A., 2000. Snake venom metalloproteinases: their role in the pathogenesis of local tissue damage. Biochimie 82, 841–850. doi:10.1016/j.toxicon.2005.06.019.

Gutiérrez, J.M., Rucavado, A., Escalante, T., Díaz, C., 2005. Hemorrhage induced by snake venom metalloproteinases: biochemical and biophysical mechanisms involved in microvessel damage. Toxicon 45, 997–1011. doi:10.1016/j.toxicon.2005.02.029.

Hochkoeppler, A., 2013. Expanding the landscape of recombinant protein production in *Escherichia coli*. Biotechnol. Lett. 35, 1971–1981. doi:10.1007/s10529-013-1396-y.

Howes, J.M., Theakston, R.D., Laing, G.D., 2007. Neutralization of the haemorrhagic activities of viperine snake venoms and venom metalloproteinases using synthetic peptide inhibitors and chelators. Toxicon 49, 734–739. doi:10.1016/j.toxicon.2006.11.020.

Jenny, R.J., Mann, K.G., Lundblad, R.L., 2003. A critical review of the methods for cleavage of fusion proteins with thrombin and factor X_a. Protein Expr. Purif. 31, 1–11. doi:10.1016/S1046-5928(03)00168-2.

Jurgelski, W., 1974. Opossum (*Didelphis virginiana Kerr*) as a biomedical model. 1. Research perspective, husbandry, and laboratory techniques. Labaratory Animal Science 24, 376–403 PMID: 4362893.

Jurgilas, P.B., Neves-Ferreira, A.G.C., Domont, G.B., Perales, J., 2003. PO41, a snake venom metalloproteinase inhibitor isolated from *Philander opossum* serum. Toxicon 42, 621–628. doi:10.1016/j.toxicon.2003.08.006.

Kilmon, J.A., 1976. High tolerance to snake venom by the Virginia opossum, *Didelphis virginiana*. Toxicon 14, 337–340. doi:10.1016/0041-0101(76)90032-5.

Komives, C.F., Balderrama, M., Cifelli, A., Sanchez, E.E., Suntravat, M., Rathore, A.S., Joshi, V., White, B., 2017. Opossum peptide that can neutralize rattlesnake venom is expressed in *Escherichia coli*. Biotechnol. Prog. 33, 81–86. doi:10.1002/btpr.2386.

Laustsen, A.H., Engmark, M., Milbo, C., Johannesen, J., Lomonte, B., Gutiérrez, J.M., Lohse, B., 2016. From fangs to pharmacology: the future of snakebite envenoming therapy. Curr. Pharmaceut. Des. 22, 5270–5293. doi:10.2174/1381612822666160623073438.

León, G., Estrada, R., Chaves, F., Rojas, G., Ovadia, M., Gutiérrez, J.M., 1998. Inhibition by CaNa2EDTA of local tissue damage induced by *Bothrops asper* (terciopelo) venom: application in horse immunization for antivenom production. Toxicon 36, 321–331. doi:10.1016/S0041-0101(97)00114-1.

León, I.R., Neves-Ferreira, A.G.C., Rocha, S.L.G., Trugilho, M.R.O., Perales, J., Valente, R.H., 2012. Using mass spectrometry to explore the neglected glycan moieties of the antiophidic proteins DM43 and DM64. Proteomics 12, 2753–2765. doi:10.1002/pmic.201200062.

Lewin, M., Samuel, S., Merkel, J., Bickler, P., 2016. Varespladib (LY315920) appears to be a potent, broad-spectrum, inhibitor of snake venom phospholipase A_2 and a possible pre-referral treatment for envenomation. Toxins 8, 248. doi:10.3390/toxins8090248.

Lipps, B.V., 1996. Lethal toxin neutralizing factor from opossum serum as a treatment for snakebites and various types of allergies. Toxicon 34, 165. doi:10.1016/0041-0101(96)83728-7.

Lipps, B.V., Lipps, F.W., 1996. Embodiments of Natural and Synthetic Lethal Toxin Neutralizing Factors and Their Utility as Treatment for Envenomation. p. 9 Cont.-in-part of U.S. Ser. No. 53,387, abandoned Patent. URL accessed (10/19/2020): https://patents.google.com/patent/US5576297A/en.

Lipps, B.V., 1999. Anti-lethal factor from opossum serum is a potent antidote for animal, plant and bacterial toxins. J. Venom. Anim. Toxins 5, 56–66. doi:10.1590/S0104-79301999000100005.

Markland, F.S., Swenson, S., 2013. Snake venom metalloproteinases. Toxicon 62, 3–18. doi:10.1016/j.toxicon.2012.09.004.

Moore, G.L., 1969. Use of azo-dye-bound collagen to measure reaction velocities of proteolytic enzymes. Anal. Biochem. 32, 122–127. doi:10.1016/0003-2697(69)90111-0.

Neves-Ferreira, A.G.C., Cardinale, N., Rocha, S.L.G., Perales, J., Domont, G.B., 2000. Isolation and characterization of DM40 and DM43, two snake venom metalloproteinase inhibitors from *Didelphis marsupialis* serum. Biochim. Biophys. Acta 1474, 309–320. doi:10.1016/S0304-4165(00)00022-2.

Neves-Ferreira, A.G.C., Perales, J., Fox, J.W., Shannon, J.D., Makino, D.L., Garratt, R.C., Domont, G.B., 2002. Structural and functional analyses of DM43, a snake venom metalloproteinase inhibitor from *Didelphis marsupialis* serum. J. Biol. Chem. 277, 13129–13137. doi:10.1074/jbc.M200589200.

Neves-Ferreira, A.G.C., Perales, J., Ovadia, M., Moussatché, H., Domont, G.B., 1997. Inhibitory properties of the antibothropic complex from the South American opossum (*Didelphis marsupialis*) serum. Toxicon 35, 849–863. doi:10.1016/S0041-0101(96)00195-X.

Nishino, N., Powers, J.C., 1980. *Pseudomonas aeruginosa* elastase. Development of a new substrate, inhibitors, and an affinity ligand. J. Biol. Chem. 255, 3482–3486 PMID: 6767718.

O'Brien, J., Lee, S.-H., Onogi, S., Shea, K.J., 2016. Engineering the protein corona of a synthetic polymer nanoparticle for broad-spectrum sequestration and neutralization of venomous biomacromolecules. J. Am. Chem. Soc. 138, 16604–16607. doi:10.1021/jacs.6b10950.

Okonechnikov, K., Golosova, O., Fursov, M., 2012. Unipro Ugene: a unified bioinformatics toolkit. Bioinformatics 28, 1166–1167. doi:10.1093/bioinformatics/bts091.

Ovadia, M., Kochva, E., 1977. Neutralization of viperidae and elapidae snake venoms by sera of different animals. Toxicon 15, 541–547. doi:10.1016/0041-0101(77)90105-2.

Perales, J., Moussatché, H., Marangoni, S., Oliveira, B., Domont, G.B., 1994. Isolation and partial characterization of an anti-bothropic complex from the serum of South American didelphidae. Toxicon 32, 1237–1249. doi:10.1016/0041-0101(94)90353-0.

Perez, J.C., Pichyangkul, S., Garcia, V.E., 1979. The resistance of three species of warm-blooded animals to western diamondback rattlesnake (*Crotalus atrox*) venom. Toxicon 17, 601–607. doi:10.1016/0041-0101(79)90234-4.

Perez, J.C., Sanchez, E.E., 1999. Natural protease inhibitors to hemorrhagins in snake venoms and their potential use in medicine. Toxicon 37, 703–728. doi:10.1016/S0041-0101(98)00205-0.

Pinto, A.F.M., Terra, R.M.S., Guimaraes, J.A., Kashiwagi, M., Nagase, H., Serrano, S.M.T., Fox, J.W., 2006. Structural features of the reprolysin atrolysin C and tissue inhibitors of metalloproteinases (TIMPs) interaction. Biochem. Biophys. Res. Commun. 347, 641–648. doi:10.1016/j.bbrc.2006.06.143.

Price, J.A., 2015. Microplate fluorescence protease assays test the inhibition of select North American snake venoms' activities with an anti-proteinase library. Toxicon 103, 145–154. doi:10.1016/j.toxicon.2015.06.020.

Rucavado, A., Escalante, T., Franceschi, A., Chaves, F., León, G., Cury, Y., Ovadia, M., Gutiérrez, J.M., 2000. Inhibition of local hemorrhage and dermonecrosis induced by *Bothrops asper* snake venom: effectiveness of early in situ administration of the peptidomimetic metalloproteinase inhibitor batimastat and the chelating agent CaNa2EDTA. Am. J. Trop. Med. Hyg. 63, 313–319. doi:10.4269/ajtmh.2000.63.313.

Rush, R.S., Mitas, M., Powers, J.C., Tanaka, T., Hersh, L.B., 1984. Fluorogenic substrates for the enkephalin-degrading neutral endopeptidase (enkephalinase). Arch. Biochem. Biophys. 231, 390–399. doi:10.1016/0003-9861(84)90402-8.

Sahdev, S., Khattar, S.K., Saini, K.S., 2008. Production of active eukaryotic proteins through bacterial expression systems: a review of the existing biotechnology strategies. Mol. Cell. Biochem. 307, 249–264. doi:10.1007/s11010-007-9603-6.

Vellard, J., 1945. Resistance of South American opossums to snake venoms. Rev. Bras. Biol. 5, 463–467.

Vellard, J., 1949. Investigaciones sobre inmunidad natural contra los venenos deserpientes I. Pub. Mus. Hist. Nat. Lima Ser A. Zool. 1, 72–96.

Vieira, S.M., Rocha, S.L.G., Neves-Ferreira, A.G.C., Almeida, R.V., Perales, J., 2017. Heterologous expression of the antimyotoxic protein DM64 in *Pichia pastoris*. PLoS Neglected Trop. Dis. 11, e0005829. doi:10.1371/journal.pntd.0005829.

Villalta-Romero, F., Borro, L., Mandic, B., Escalante, T., Rucavado, A., Gutiérrez, J.M., Neshich, G., Tasic, L., 2017. Discovery of small molecule inhibitors for the snake venom metalloprotease BaP1 using *in silico* and *in vitro* tests. Bioorg. Med. Chem. Lett. 27, 2018–2022. doi:10.1016/j.bmcl.2017.03.007.

Villalta-Romero, F., Gortat, A., Herrera, A.E., Arguedas, R., Quesada, J., de Melo, R.L., Calvete, J.J., Montero, M., Murillo, R., Rucavado, A., Gutiérrez, J.M., Pérez-Payá, E., 2012. Identification of new snake venom metalloproteinase inhibitors using compound screening and rational peptide design. Am. Chem. Soc. Med. Chem. Letters 3, 540–543. doi:10.1021/ml300068r.

Voss, R.S., Jansa, S.A., 2012. Snake-venom resistance as a mammalian trophic adaptation: lessons from didelphid marsupials. Biol. Rev. 87, 822–837. doi:10.1111/j.1469-185X.2012.00222.x.

Warrell, D.A., 2010. Snake bite. Lancet 375, 77–88. doi:10.1016/S0140-6736(09)61754-2.

Waugh, D.S., 2011. An overview of enzymatic reagents for the removal of affinity tags. Protein Expr. Purif. 80, 283–293. doi:10.1016/j.pep.2011.08.005.

Werner, R.M., Vick, J.A., 1976. Resistance of the opossum (*Didelphis virginiana*) to envenomation by snakes of the crotalidae family. In: Edgewood Arsenal Technical Report (Aberdeen Proving Grounds, MD. Edgewood Arsenal Biomedical Laboratory), pp. 1–19 URL accessed (10/19/2020): https://apps.dtic.mil/dtic/tr/fulltext/u2/a034590.pdf.

Werner, R.M., Vick, J.A., 1977. Resistance of the opossum (*Didelphis virginiana*) to envenomation by snakes of the family crotalidae. Toxicon 15, 29–32. doi:10.1016/0041-0101(77)90066-6.

Werner, R.M., Faith, R.E., 1978. Decrease in the lethal effect of snake venom by serum of the opossum, *Didelphis marsupialis*. Lab. Anim. Sci. 28, 710–713 PMID: 750730.

Williams, D., Gutiérrez, J.M., Harrison, R., Warrell, D.A., White, J., Winkel, K.D., Gopalakrishnakone, P., 2010. The global snake bite initiative: an antidote for snake bite. Lancet 375, 89–91. doi:10.1016/S0140-6736(09)61159-4.

Williams, H.F., Layfield, H.J., Vallance, T., Patel, K., Bicknell, A.B., Trim, S.A., Vaiyapuri, S., 2019. The urgent need to develop novel strategies for the diagnosis and treatment of snakebites. Toxins 11, 363. doi:10.3390/toxins11060363.

World Health Organization, 2007. Rabies and Envenomings: A Neglected Public Health Issue, Report of a Consultative Meeting. pp. 1–31 URL accessed (10/19/2020): http://www.who.int/bloodproducts/animal_sera/Rabies.pdf.

World Health Organization, 2010. Who Guidelines for the Production, Control and Regulation of Snake Antivenom Immunoglobulins. 1-192. URL accessed (10/19/20): https://www.who.int/bloodproducts/snake_antivenoms/snakeantivenomguide/en/.

Yang, H., Liu, L., Xu, F., 2016. The promises and challenges of fusion constructs in protein biochemistry and enzymology. Appl. Microbiol. Biotechnol. 100, 8273–8281. doi:10.1007/s00253-016-7795-y.